

1 **Fibronectin binding proteins SpsD and SpsL both support invasion of canine epithelial cells**  
2 **by *Staphylococcus pseudintermedius***

3  
4 *Staphylococcus pseudintermedius* internalization

5  
6 **Giampiero Pietrocola<sup>1</sup>, Valentina Gianotti<sup>1\*</sup>, Amy Richards<sup>2\*</sup>, Giulia Nobile<sup>1</sup>, Joan A.**  
7 **Geoghegan<sup>3</sup>, Simonetta Rindi<sup>1</sup>, Ian R. Monk<sup>3</sup>, Andrea S. Bordt<sup>4</sup>, Timothy J. Foster<sup>3</sup>, J. Ross**  
8 **Fitzgerald<sup>2</sup> and Pietro Speziale<sup>1#</sup>**

9  
10 1 Department of Molecular Medicine, Unit of Biochemistry, Viale Taramelli 3/b, 27100 Pavia, Italy

11 2 The Roslin Institute and Edinburgh Infectious Diseases, University of Edinburgh, Easter Bush,  
12 Midlothian EH25 9RG, Scotland, UK

13 3 Department of Microbiology, Moyne Institute of Preventive Medicine, Trinity College Dublin,  
14 Dublin 2, Ireland

15 4 Center for Infectious and Inflammatory Diseases, Texas A&M Health Science Center, MS 1201  
16 2121 W Holcombe Blvd Houston, TX 77030-3303

17  
18 \* These authors contributed equally to this work

19  
20 #Address correspondence to Pietro Speziale,

21 E-mail: pspeziale@unipv.it

22 Tel: 0039 0382 987787

23 Fax: 0039 0382 423108

24

25

26

27 **Abbreviations:** BHI, brain heart infusion; BSA, bovine serum albumin; CFU, colony forming unit;  
28 CGP77675, 5,7-diphenyl-pyrrolo(2,3-d)pyrimidine; CPEK, canine progenitor epidermal  
29 keratinocytes; DMEM, high-glucose Dulbecco's modified Eagle's medium; DMSO, dimethyl  
30 sulphoxide; FBS, fetal bovine serum; Fn, fibronectin; FnBPA/B, fibronectin binding protein A/B;  
31 GBD, gelatin-binding domain of fibronectin; HaCaT, cultured human keratinocyte; Hep-2, human  
32 epithelial cell line; LA, Luria agar; LB, Luria broth; MTT, [3-(4,5-dimethylthiazol-2-yl)-2,5-  
33 diphenyltetrazolium bromide]; N29, N-terminal fragment of fibronectin; PP2, 4-amino-5-(4-  
34 chlorophenyl)-7-(*t*-butyl)pyrazolo[3,4-*d*]pyrimidine; PP3, 1-phenyl-1*h*-pyrazolo[3,4-*d*]pyrimidin-4-  
35 amine; PVL, panton-valentine leucocidin; RGD, serine-glycine aspartate peptide; RGE, serine-  
36 glycine-glutamic acid peptide; SpsD/SpsL, *Staphylococcus pseudintermedius* surface protein D/L.

37  
38  
39  
40  
41  
42  
43  
44  
45  
46  
47  
48  
49  
50  
51  
52

## 53 ABSTRACT

54 In this study we investigated the cell wall-anchored fibronectin-binding proteins SpsD and  
55 SpsL from the canine commensal and pathogen *Staphylococcus pseudintermedius* for their  
56 role in promoting bacterial invasion into canine keratinocyte CPEK cells. Invasion was  
57 examined by the gentamicin protection assay and fluorescence microscopy. An *spsD/spsL*  
58 double mutant of strain ED99 had a dramatically reduced capacity to invade CPEK cell  
59 monolayers, while no difference in the invasion level was observed with single mutants. *L.*  
60 *lactis* transformed with plasmids expressing SpsD and SpsL promoted invasion showing that  
61 both proteins are important. Soluble fibronectin was required for invasion and an RGD-  
62 containing peptide or antibodies recognizing the integrin  $\alpha_5\beta_1$  markedly reduced invasion,  
63 suggesting an important role for the integrin in this process. Src kinase inhibitors effectively  
64 blocked internalization suggesting a functional role for the kinase in invasion. In order to  
65 identify the minimal fibronectin-binding region of SpsD and SpsL involved in the  
66 internalization process, recombinant fragments of both proteins were produced. The SpsD<sub>520-</sub>  
67 <sub>846</sub> and SpsL<sub>538-823</sub> regions harbouring the major fibronectin-binding sites inhibited *S.*  
68 *pseudintermedius* internalization. Finally, the effects of staphylococcal invasion on the  
69 integrity of different cell lines was examined. Because SpsD and SpsL are critical factors for  
70 adhesion and invasion, blocking these processes could provide a strategy for future  
71 approaches to treating infections.

72

73 Key words: *Staphylococcus*, adhesin, fibronectin, invasion, keratinocyte

74

75

76

77

78

79 **INTRODUCTION**

80 The Gram-positive bacterium *Staphylococcus pseudintermedius* is a common commensal of dogs  
81 (1, 2). The bacterium is also the most common pathogen associated with canine otitis externa and  
82 pyoderma as well as surgical wound infections and urinary tract infections (3). Sporadic cases of  
83 human infection have also been reported, including individuals exposed to colonized household pets  
84 (4-7). Genome sequence analysis (8, 9) indicated that *S. pseudintermedius* could encode many  
85 potential virulence factors including toxins, enzymes and surface proteins, some of which can  
86 promote adhesion of the bacterium to the surface of epithelial cells (10-13) and to components of  
87 the extracellular matrix (14,15)

88 Two cell wall-anchored surface proteins that are likely to be important in host tissue  
89 colonization and pathogenesis are SpsD and SpsL (Fig.1) (15). The primary translation product of  
90 SpsD from strain ED99 has an N-terminal secretory signal sequence and a C-terminal cell wall-  
91 anchoring domain (the sorting signal) comprising an LPXTG motif, a hydrophobic trans-membrane  
92 domain and a short sequence rich in positively charged residues. Residues at the N-terminus of  
93 SpsD are 40% identical to the fibrinogen-binding A domain of FnBPB from *S. aureus* and are  
94 predicted to fold into three subdomains N1, N2 and N3. This domain is followed by a connecting  
95 region C and a repeat region R. SpsL includes a signal sequence at the N terminus followed by an A  
96 domain with two IgG-like folds (N2 and N3), a domain containing seven tandem repeats with weak  
97 homology to the fibronectin binding repeats of FnBPA from *S. aureus* and a C-terminal sorting  
98 signal.

99 SpsD and SpsL mediate bacterial adherence to fibrinogen (15) and fibronectin (Fn) (15),  
100 while SpsD also binds to cytokeratin 10 and elastin (16). The binding site in fibrinogen for SpsD  
101 was mapped to residues 395-411 in the  $\gamma$ -chain, while a binding site for SpsD in Fn was localized to  
102 the N-terminal region. SpsD also binds to glycine-and serine-rich omega loops within the C-  
103 terminal tail region of cytokeratin 10 (16).

104 Another important Sps protein involved in the host colonization is SpsO, that has been  
105 demonstrated to mediate adherence to *ex vivo* canine keratinocytes (12). However, the host  
106 ligand(s) interacting with SpsO remain to be determined (15).

107 The SpsO protein of *S. pseudintermedius* is also likely to be involved in colonization of the  
108 canine host. It promotes adhesion to *ex vivo* canine corneocytes, as does SpsD, although the  
109 ligand(s) recognized by SpsO remain to be identified. Invasive bacteria actively induce their own  
110 uptake by phagocytosis into normally non-phagocytic cells where they establish a protected niche  
111 within which they can replicate (17). For example, *S. aureus*, usually considered an extracellular  
112 pathogen, can invade a variety of non-professional phagocytic cells explaining its capacity to  
113 colonize mucosa and its persistence in tissue after bacteraemia. The underlying major molecular  
114 mechanism of invasion involves the Fn-binding adhesins FnBPA and FnBPB (18,19). Fn-bridging  
115 between FnBPs and  $\alpha 5\beta 1$  integrins on the host cell surface is sufficient to induce zipper-type uptake  
116 of staphylococci (18-20). The ternary complex promotes integrin clustering and a relay of signals  
117 that result in cytoskeletal rearrangements. The rearrangements are accompanied by endocytosis of  
118 *S. aureus* and internalization (17).

119 In this study we wished to investigate whether *S. pseudintermedius* shares with *S. aureus* the  
120 ability to invade non-professional phagocytic cells and to determine the bacterial and host  
121 components that are involved. We reasoned that both SpsD and SpsL could be involved in the  
122 internalization of *S. pseudintermedius* by host cells. The objective of this study was to investigate  
123 internalization and its mechanistic basis. The analysis of this process will provide insights into the  
124 potential of a vaccine comprising components of SpsD and SpsL for the prevention of canine  
125 pyoderma.

126

## 127 **MATERIALS AND METHODS**

### 128 **Bacterial strains and culture conditions.**

129 *S. pseudintermedius* strain ED99 (formerly M732 / 99) was isolated from a canine bacterial  
130 pyoderma case presented to the Dermatology Service of The Hospital for Small Animals, Division  
131 of Veterinary Clinical Sciences, The Royal (Dick) School of Veterinary Studies, The University of  
132 Edinburgh. *S. pseudintermedius* strains 264, 324, 326, 327, 328 and 329 were isolated from cases of  
133 canine pyoderma and were a kind gift from Dr. Neil McEwan, University of Liverpool. *S.*  
134 *pseudintermedius* strains 81852, 91180, 253834, 237425, 235214/1 were isolated from cases of  
135 canine pyoderma and were donated from Istituto Zooprofilattico Sperimentale della Lombardia e  
136 della Emilia Romagna, Pavia, Italy. The strains were classified as *S. pseudintermedius* using  
137 standard phenotypic tests (21). *S. pseudintermedius* ED99 and its mutants were grown in Brain  
138 Heart Infusion (BHI) (VWR International Srl, Milan, Italy) at 37°C with shaking. Transformants of  
139 *Lactococcus lactis* harbouring plasmid pOri23, pOri23::*spsD* or pOri23::*spsL* (15) were grown in  
140 M17 medium (Difco, Detroit, MI, USA) supplemented with 10% lactose, 0.5% glucose and 10 µg  
141 ml<sup>-1</sup> erythromycin at 30°C without shaking. *Escherichia coli* DC10B (22) and TOPP3 (Stratagene,  
142 La Jolla, CA) were grown in Luria agar (LA) and Luria broth (LB) (VWR International Srl).

143 **Reagents, proteins and antibodies.** Human fibronectin was purified from plasma by a  
144 combination of gelatin- and arginine-Sepharose affinity chromatography. The purity of the protein  
145 was assessed by 7.5% SDS-PAGE and Brilliant Blue Coomassie staining. To exclude the  
146 possibility of trace amounts of contaminants, affinity purified fibronectin was spotted onto  
147 nitrocellulose membranes at different concentrations and overlaid with anti-fibrinogen and anti-  
148 plasminogen antibodies (23). The N-terminal fragment of Fn (N29) containing the five N-terminal  
149 type I modules, and the gelatin-binding domain (GBD) consisting of four type I modules and two  
150 type II modules were isolated as previously reported (24). Unless stated otherwise all reagents were  
151 purchased from Sigma-Aldrich (St Louis, MO, USA). The anti-human Fn rabbit polyclonal IgG  
152 was purchased from Pierce (Rockford, IL, USA). The mouse monoclonal antibody JBS5 against the  
153 human integrin  $\alpha 5\beta 1$  was purchased from Merck-Millipore (Darmstadt, Germany). The rabbit  
154 polyclonal antibody against the  $\alpha 5$  chain of the  $\alpha 5\beta 1$  integrin, the mouse monoclonal antibodies

155 BV7 against the human  $\beta 1$  chain and B212 against the human  $\beta 3$  chain of the integrin  $\alpha v\beta 3$  were a  
156 generous gift of Prof. G. Tarone (University of Turin, Italy). Mouse polyclonal antibodies against  
157 region A of SpsD and SpsL were prepared as previously reported (16).

158 **DNA manipulation.** DNA encoding regions SpsD<sub>164-523</sub>, SpsD<sub>520-846</sub>, SpsD<sub>844-960</sub>, SpsL<sub>220-531</sub>, and  
159 SpsL<sub>538-823</sub> were amplified by PCR using *S. pseudintermedius* ED99 genomic DNA as the template.  
160 Oligonucleotides were purchased from Integrated DNA Technologies (Leuven, Belgium) (see  
161 Table S1 in the supplemental material). Restriction enzyme cleavage sites (see Table S1) were  
162 incorporated at the 5' ends of the primers to facilitate cloning into plasmid pQE30 (Qiagen,  
163 Chatsworth, CA, USA). Restriction enzymes were purchased from New England Biolabs  
164 (Hertfordshire, UK). The integrity of cloned DNA was confirmed by sequencing (Primmbiotech,  
165 Milan, Italy).

166 **Expression and purification of recombinant proteins.** Recombinant proteins were expressed  
167 from pQE30 in *E. coli* TOPP3 (Stratagene). Overnight starter cultures were diluted 1:50 in LB  
168 containing ampicillin ( $100 \mu\text{g ml}^{-1}$ ) and incubated with shaking until the culture reached  $\text{OD}_{600\text{nm}}$   
169 0.4-0.6. Recombinant protein expression was induced by addition of isopropyl 1-thio- $\beta$ -D-  
170 galactopyranoside (0.5 mM) and continued for 2 h. Bacterial cells were harvested by centrifugation  
171 and frozen at  $-80^\circ\text{C}$ . Recombinant proteins were purified from cell lysates by  $\text{Ni}^{2+}$  affinity  
172 chromatography on a HiTrap chelating column (GE Healthcare, Buckinghamshire, UK). Protein  
173 purity was assessed to be 98% by SDS-PAGE and Brilliant Blue Coomassie staining and  
174 densitometric analysis.

175 **ELISA-type solid phase binding assays.** The ability of immobilized recombinant proteins to  
176 interact with soluble human Fn was determined using ELISA assays. Microtiter wells were coated  
177 overnight at  $4^\circ\text{C}$  with  $100 \mu\text{l}$  of  $10 \mu\text{g ml}^{-1}$  of bacterial protein in 50 mM sodium carbonate, pH 9.5.  
178 To block additional protein-binding sites, the wells were treated for 1h at  $22^\circ\text{C}$  with  $200 \mu\text{l}$  of 2%  
179 BSA in PBS. The plates were then incubated for 1 h with increasing amounts of Fn. One microgram

180 of the specific anti-Fn rabbit IgG (1:2000) in PBS with 0.1% BSA was added to the wells, followed  
181 by incubation for 90 min. After washing, the plates were incubated for 1 h with peroxidase-  
182 conjugated secondary anti-rabbit IgG diluted 1:1000. After washing, *o*-phenylenediamine  
183 dihydrochloride was added and the absorbance at 490 nm was determined. To calculate the relative  
184 affinity association constant ( $K_A$ ) values of each bacterial protein for Fn the following equation was  
185 employed:  $A = A_{\max}[L]K_A/(1 + K_A[L])$ , where [L] is the molar concentration of ligand. The  
186 dissociation constants ( $K_D$  values) were calculated as reciprocals of the  $K_A$  values. The assays were  
187 performed at least 3 times for each protein.

188 **Construction of *spsD* and *spsL* null mutants.** Allele replacement mutagenesis of *spsD* and *spsL*  
189 was performed using the thermosensitive plasmids pIMAY and pIMAY-Z (Table 1). For generation  
190 of the *spsD* null mutation, approximately 500 bp fragments of DNA flanking the gene were PCR-  
191 amplified using the AB and CD primers, spliced together and cloned into the blunt end ligation  
192 pSC-B vector (StrataClone, Agilent Technologies, Santa Clara, CA) before subcloning into pIMAY  
193 to produce the pIMAY  $\Delta$ *spsD* construct. The plasmid was transformed into *E. coli* DC10B before  
194 being electro-transformed into *S. pseudintermedius* ED99 at 28°C selecting on 10  $\mu$ g ml<sup>-1</sup>  
195 chloramphenicol, as previously described for *S. aureus* (25). For generation of the *spsL* null  
196 mutation, a sequence ligase independent cloning (SLIC) protocol was performed (26) using  
197 pIMAY-Z, a derivative of pIMAY with a constitutive *lacZ* marker, to construct pIMAY-Z  $\Delta$ *spsL*.  
198 Once the plasmids were transformed into ED99 at 28°C, growth at the restrictive temperature of  
199 37°C selected for integrants. OUT primers, located outside of the flanking regions and gene of  
200 interest, were used to determine if integration had occurred upstream or downstream of the  
201 chromosomal gene (22). A single colony from each site of integration was inoculated into broth and  
202 grown at 28°C then diluted and grown at 37°C. The *S. aureus* antisense *secY* mechanism within  
203 pIMAY (27) was non-functional in *S. pseudintermedius* and the *lacZ* marker was ineffective



204 because plasmid-free cells expressed endogenous  $\beta$ -galactosidase activity. Allele exchange was  
205 confirmed using OUT primer PCR and sequencing the resultant fragment (see Table S2).

206 **Release of surface proteins from *S. pseudintermedius* and *L. lactis*.** *S. pseudintermedius* and *L.*  
207 *lactis* cells were grown to OD<sub>600nm</sub> of 0.4-0.6. Cells were harvested by centrifugation at 7000 x g at  
208 4°C for 15 min, washed 3 times with PBS and resuspended at an OD<sub>600nm</sub> of 40 in lysis buffer (50  
209 mM Tris-HCl, 20 mM MgCl<sub>2</sub>, pH 7.5) supplemented with 30% raffinose. Cell wall proteins were  
210 solubilized from *S. pseudintermedius* by incubation with lysostaphin (200  $\mu$ g ml<sup>-1</sup>) and from *L.*  
211 *lactis* with mutanolysin (1000 U/ml) and lysozyme (900  $\mu$ g ml<sup>-1</sup>) at 37°C for 20 min in the presence  
212 of protease inhibitors (Complete Mini TM; Roche Molecular Biochemicals, Indianapolis, IN, USA).  
213 Protoplasts were recovered by centrifugation at 6000 x g for 20 min, and the supernatants were  
214 taken as the wall fractions. The material obtained from *S. pseudintermedius* ED99 and its mutants  
215 were adsorbed on IgG-sepharose columns before Western immunoblotting analysis to remove IgG-  
216 binding proteins that would otherwise interfere with the specific antibody staining.

217 **SDS-PAGE and Western immunoblotting.** Samples for analysis by SDS-PAGE were boiled for 5  
218 min in sample buffer [0.125 M Tris-HCl, 4% (w/v) SDS, 20% (v/v) glycerol, 10% (v/v)  $\beta$ -  
219 mercaptoethanol, 0.002% (w/v) bromophenol blue] and separated on 10% (w/v) polyacrylamide  
220 gels. The gels were stained with Coomassie Brilliant Blue (BioRad, Hercules, CA, USA). For  
221 Western immunoblotting, material was subjected to SDS-PAGE and then electroblotted onto a  
222 nitrocellulose membrane (GE Healthcare). The membrane was blocked overnight at 4°C with 5%  
223 (w/v) skim milk in PBS, washed, and incubated with mouse polyclonal antibody against region A of  
224 SpsD or SpsL (1  $\mu$ g ml<sup>-1</sup>) for 1 h at 22°C. Following additional washings with 0.5% (v/v) Tween 20  
225 in PBS (PBST), the membrane was incubated for 1 h with horseradish peroxidase-conjugated rabbit  
226 anti-mouse IgG. Finally, blots were developed using the ECL Advance Western Blotting Detection  
227 Kit (GE Healthcare) and an ImageQuantTM LAS 4000 mini Biomolecular Imager (GE  
228 Healthcare).

229 **Mammalian cell lines and culture conditions.** Canine progenitor epidermal keratinocytes (CPEK)  
230 cells were cultured in *CnT-0.9* medium (CELLnTEC, Bern, Switzerland), without antibiotics at  
231 37°C in 5% CO<sub>2</sub>. The spontaneously immortalised keratinocyte (HaCaT) and the human epithelial  
232 cell line HEp-2 were cultured in high-glucose Dulbecco's modified Eagle's medium (DMEM)  
233 (Gibco BRL, Rockville, MD, USA) supplemented with 10% heat-inactivated fetal bovine serum  
234 (FBS) (EuroClone, Milan, Italy), 2% penicillin and streptomycin, 2% sodium pyruvate, 2% L-  
235 glutamine at 37°C in 5% CO<sub>2</sub>. Cells were cultured in T75 flasks to approximately 95% confluency,  
236 liberated with trypsin-EDTA (EuroClone), resuspended in invasion medium (growth medium  
237 without antibiotics) and plated as reported below in the cell invasion assay.

238 **Cell invasion assay.** Cell invasion assays were performed (28) with modifications. Briefly, cells  
239 were plated at  $5 \times 10^5$  (in 0.4 ml invasion medium) into 24 well plates (Corning) and allowed to  
240 attach for 24 h at 37°C. Staphylococcal cultures were grown overnight in BHI at 37°C with shaking.  
241 *L. lactis* was grown overnight in M17 broth at 30°C without shaking. The following day, cultures  
242 were diluted 1:40 in fresh BHI or M17 medium, respectively, and grown to an OD<sub>600nm</sub> of 0.4, were  
243 washed 3 times in PBS and diluted to obtain  $10^7$  cells/ml in *CnT-BM.2* supplemented with 10% FBS  
244 + 2 mM L-glutamine. Bacterial suspensions (1 ml) were added to each well and the plates incubated  
245 for 2 h at 37°C. Monolayers were then washed 3 times in PBS to remove unattached bacteria.  
246 Media containing antibiotics (200 µg ml<sup>-1</sup> gentamicin + 2% penicillin and streptomycin) was added  
247 and the plate incubated for an additional 2 h to kill extracellular bacteria. The wells were washed  
248 again, and internalized bacteria released by incubating with 200 µl of H<sub>2</sub>O containing 0.1% v/v  
249 Triton-X 100. Serial dilutions of the cell lysates were plated in duplicate on BHI agar and CFU  
250 were counted after incubation. All assays were carried out in triplicate. Samples of monolayers were  
251 lysed prior to inoculation, plated on BHI agar and the absence of staphylococcal colonies noted.

252 **Inhibition of invasion.** The Src family kinase inhibitors PP2, PP3 and CGP77675 (25 µM) were  
253 dissolved in dimethyl sulphoxide (DMSO), added to the cell media at the indicated concentrations

254 and preincubated with monolayers for 1 h at 37°C in 5% CO<sub>2</sub> before addition of bacteria. Likewise,  
255 wortmannin (20 nM), genistein (200 μM) and cytochalasin D (50 μM) were dissolved in PBS and  
256 incubated with cells for 60 min prior to the addition of bacteria. Gentamicin protection assays were  
257 then performed as described above except no intermediate washing was carried out. To test cell  
258 viability during exposure to the Src inhibitors the compounds were added to cell monolayers for 3 h  
259 at 37°C. Then the cells were gently washed with DMEM, trypsinized and mixed with an equal  
260 volume of trypan blue (0.5% (v/v) in PBS) for 5 min. Ten microliters of the mixture were placed on  
261 a Neubauer chamber and stained cells were counted by light microscopy. The percentage of dead  
262 cells was calculated by dividing the mean number of dead (stained) cells by the total number of  
263 cells in 50 microscopic fields, and multiplying by 100.

264 **Fluorescence microscopy.** Bacteria were grown to an OD<sub>600nm</sub> of 0.3 (*S. pseudintermedius*) or 0.4  
265 (*L. lactis* centrifuged resuspended in 100 μl PBS. Then 0.5 μl 10 mM calcein-AM (Molecular  
266 Probes, Eugene, OR, USA) was added and incubated for 1 h at 37°C (*S. pseudintermedius*) or 2 h  
267 at 30°C (*L. lactis*). Stained bacteria were washed 3 times with PBS and resuspended in 1 ml PBS.  
268 Suspensions (100 μl) were added to CPEK monolayers and incubated for 2 h at 37°C to allow  
269 internalization. Cells were washed with PBS, counterstained for 1–3 min with ethidium bromide (10  
270 μg ml<sup>-1</sup>) and washed again. Fluorescence microscopy (Olympus BX51; Olympus, Segrate, Italy)  
271 was performed using a green filter, a red filter, and white light. Images were captured with a CCD  
272 camera and assembled using Adobe Photoshop Creative Suite 2.

273 **Staining of monolayers.** Mammalian cells were stained with Giemsa Stain Modified Solution  
274 (Sigma) according to the manufacturer's instructions and observed under a light microscope at 20 x  
275 magnification.

276 **Invasion assays with formaldehyde-fixed staphylococci.** To perform invasion assays with killed  
277 bacteria, staphylococci were fixed in 0.5% formaldehyde in PBS for 1 h, stained with Calcein-AM  
278 and subjected to fluorescence microscopy. Alternatively, to analyze the effect of formaldehyde-

279 fixed staphylococci on cell survival, monolayers were stained with Giemsa and observed as  
280 reported above.

281 **MTT assay.** The MTT tetrazolium reduction assay was performed according to the manufacturer's  
282 instructions (Sigma).

283 **Statistical methods.** Continuous data were expressed as means and standard deviations. Two-group  
284 comparisons were performed by Student's *t* test. One-way analysis of variance, followed by  
285 Bonferroni's post hoc tests, was exploited for comparison of three or more groups. Analyses were  
286 performed using Prism 4.0 (GraphPad). Two-tailed *P* values of 0.001 were considered statistically  
287 significant.

288

## 289 RESULTS

290 **SpsD and SpsL binding to fibronectin.** To localize the Fn-binding sites in SpsD and SpsL,  
291 recombinant domains were obtained following PCR amplification of genomic DNA from strain  
292 ED99. The cloned SpsD domains included the minimum fibrinogen-binding region (residues 164-  
293 523) (SpsD<sub>164-523</sub>), a connecting region C (residues 520-846) (SpsD<sub>520-846</sub>) and a repeat region R  
294 (residues 844-960) (SpsD<sub>844-960</sub>). Two recombinant SpsL domains were expressed: the N-terminal  
295 region encompassing residues 220-531 (SpsL<sub>220-531</sub>) and the repetitive domain spanning 538-823  
296 (SpsL<sub>538-823</sub>). As shown in ELISA-type solid phase binding assays (Fig. 2) recombinant SpsD<sub>520-846</sub>  
297 and SpsL<sub>538-823</sub> regions bound Fn dose-dependently and saturably, while no binding was exhibited  
298 by SpsL<sub>220-531</sub> and SpsD<sub>844-960</sub>. SpsD<sub>520-846</sub> and SpsL<sub>538-823</sub> domains bound Fn in the low nanomolar  
299 range (SpsD<sub>520-846</sub>  $K_D = 1.7 \pm 0.38$ , SpsL<sub>538-823</sub>  $K_D = 0.81 \pm 0.02$  nM) while SpsD<sub>164-523</sub> gave a half  
300 maximal binding of  $2.19 \pm 0.47$   $\mu$ M (data not shown).

## 301 Invasion of mammalian cells by *S. pseudintermedius*.

302 Several *S. pseudintermedius* isolates were found to invade canine keratinocyte-derived CPEK cells.

303 The magnitude of invasion was very similar to or even higher than that of the archetypal invasive *S.*

304 *aureus* strain Cowan 1 (Fig. 3). Thus, invasion of CPEK cells is a general property of *S.*  
305 *pseudintermedius*.

306 **Requirement for fibronectin for efficient invasion by *S. pseudintermedius* ED99.** To investigate  
307 the role of soluble plasma-derived Fn in invasion, FBS was passed over a gelatin-Sepharose column  
308 to remove soluble Fn before being used in the invasion assay. An 85 % reduction in the level of  
309 invasion of CPEK cells was observed when the Fn-depleted FBS was used in the invasion medium  
310 compared to unadsorbed FBS. The addition of human Fn to a final concentration of  $1\mu\text{g ml}^{-1}$  was  
311 sufficient to restore the level of invasion to that observed in the presence of whole FBS (Fig. 4A).  
312 This suggests that *S. pseudintermedius* strain ED99 can use soluble plasma-derived Fn in the  
313 invasion process. Removal of FBS from the assay reduced the invasion level by 95%, suggesting  
314 that additional minor components in the FBS other than Fn might contribute. However, although  
315 removal of Fn from the gelatin-adsorbed FBS was shown by ELISA and Western blotting, residual  
316 internalization can be due to trace amounts of Fn remaining in the invasion medium.

317 When bacteria were preincubated with increasing amounts of the N29 fragment of Fn and  
318 then tested for adherence to or invasion of CPEK cells, we observed an almost complete inhibition  
319 of bacterial internalization. Conversely, no effect was observed when the invasion assay was  
320 performed with a high concentration of the GBD of Fn (Fig. 4B). Together these findings indicate  
321 that the N29 domain is specifically involved in adhesion to and invasion of CPEK cells.

322 **Invasion of CPEK cells by ED99 mutants and *L. lactis* expressing SpsD or SpsL.** Mutants of *S.*  
323 *pseudintermedius* ED99 deficient in SpsD and SpsL were tested for their ability to attach to surface-  
324 coated Fn. Mutants defective in either SpsD or SpsL alone adhered equally as well as the parental  
325 strain while the double mutant defective in both proteins did not bind at all (data not shown). The  
326 absence of SpsD or SpsL proteins was confirmed by testing material solubilized from the cell wall  
327 with lysostaphin by Western blotting and probing with antibodies against region A of SpsD or  
328 SpsL. Both the proteins were absent from the double mutant (Fig. 5A). Conversely, SpsL was  
329 expressed normally by the SpsD mutant and *vice versa*.

330 The SpsD and SpsL defective mutants were also tested for invasiveness. Single mutants  
331 retained the ability to invade CPEK cells at the same level as the wild type, while the double mutant  
332 lacking both SpsD and SpsL invaded at a much lower level (Fig. 5B).

333 In order to test whether co-receptors are required for SpsD or SpsL-mediated invasion, we  
334 expressed both *S. pseudintermedius* proteins individually in *Lactococcus lactis* (Fig 6A).  
335 Transformants of *L. lactis* carrying plasmid pOri23::*spsD* and pOri23::*spsL* (Fig. 6A) showed  
336 invasiveness similar to that of the wild type strain ED99 (Fig. 5B), while very low internalization  
337 by CPEK cells was observed with *L. lactis* harboring the empty plasmid (Fig. 6B).

338 Reduced invasion by the double mutant of ED99 was also assessed by visualizing uptake  
339 into CPEK cells by fluorescent imaging. Bacteria were stained with calcein-AM (green) prior to  
340 CPEK cell invasion and at the assay end-point the fluorescence of external bacteria was visualized  
341 with ethidium bromide (red). As shown in Fig. 5 C, the wild type and the single mutant strains were  
342 observed inside CPEK cells, while no green fluorescence, indicative of the internalized bacteria,  
343 was detected when the double mutant was tested. *L. lactis* expressing SpsL or SpsD behaved  
344 similarly (Fig. 6C). Together these results demonstrate that expression of a single adhesin (SpsD or  
345 SpsL) is sufficient to confer efficient uptake of bacteria into CPEK cells.

346 **Localization of Sps domains promoting invasion of CPEK cells.** To identify the domains of  
347 SpsD and SpsL that are involved in invasion, recombinant fragments were assessed for inhibition of  
348 *S. pseudintermedius* ED99 uptake into CPEK cells. We found that SpsD<sub>520-846</sub> (Fig.7A) and SpsL<sub>538-</sub>  
349 <sub>823</sub> (Fig. 7B) strongly inhibited internalization, whereas SpsD<sub>164-523</sub> showed a weak inhibitory effect.  
350 The inhibitory effects exhibited by these proteins correlates with their affinities for fibronectin.  
351 SpsL<sub>220-631</sub> and SpsD<sub>844-960</sub> when used at the same concentrations did not interfere with  
352 staphylococcal invasion.

353 **Dependence of invasion on integrin  $\alpha_5\beta_1$ .** Immunofluorescent antibodies that specifically bind to  
354 the  $\alpha_5$  subunit of the human Fn-binding  $\alpha_5\beta_1$  integrin stained CPEK cells, suggesting that the  
355 canine cells express an  $\alpha_5\beta_1$  integrin that is closely related to the human integrin (Fig. 8A, inset). To

356 test the role of the  $\alpha_5\beta_1$  integrin in invasion, CPEK cells were preincubated with function-blocking  
357 anti- $\alpha_5\beta_1$  IgG prior to adding *S. pseudintermedius*. Antibodies recognizing the  $\alpha_5$  and the  $\beta_1$  chains  
358 both reduced internalization of *S. pseudintermedius* by more than 80%, whereas antibodies against  
359 the  $\beta_3$  chain of the human  $\alpha_v\beta_3$  integrin did not alter invasion (Fig. 8A). This indicates that the  $\alpha_5\beta_1$   
360 integrin on canine CPEK cells is responsible for Fn-mediated bacterial invasion.

361 **Inhibition of invasion by an RGD-containing peptide.** The  $\alpha_5\beta_1$  integrin recognizes the tripeptide  
362 sequence RGD within the cell-binding domain of Fn (29, 30). To investigate the role of this  
363 interaction in invasion of *S. pseudintermedius*, the effect of the RGDS peptide was analyzed.  
364 Incubation of CPEK cells with the RGDS peptide reduced the level of invasion by strain ED99 in a  
365 dose-dependent manner, while a control peptide RGES had no inhibitory effect (Fig. 8B). This  
366 suggests that the interaction of  $\alpha_5\beta_1$  with Fn is necessary for efficient invasion of CPEK cells.

367 **Protein phosphorylation during *S. pseudintermedius* invasion.** To identify changes in host cell  
368 signalling associated with staphylococcal invasion, the assay was performed in the presence of  
369 protein tyrosine phosphorylation inhibitors. Genistein, a tyrosine kinase inhibitor, strongly inhibited  
370 internalization, whereas wortmannin, an inhibitor of the phosphatidylinositol-3-phosphate kinase,  
371 did not (Fig. 8C). We also tested Src kinase inhibitors and found that both CGP77675 and PP-2  
372 inhibited *S. pseudintermedius* internalization into CPEK cells. While both inhibitors effectively  
373 blocked internalization, CGP77675 appeared to be a more potent inhibitor compared to PP-2. PP-3,  
374 a compound similar to PP-2 but with no significant Src inhibitory activity, had no effect on  
375 internalization (Fig. 8C). At the concentrations used the inhibitors did not affect bacterial adhesion  
376 to the CPEK cells or cause loss of viability as shown by Trypan blue staining (data not shown). To  
377 investigate a possible role for actin cytoskeleton rearrangements in *S. pseudintermedius* invasion,  
378 we tested cytochalasin D which interferes with F-actin polymerization. Pre-treatment of CPEK cells  
379 with 1 $\mu$ g/ml cytochalasin D almost completely abolished invasion demonstrating the involvement  
380 of actin cytoskeletal rearrangements (Fig. 8C).

381 **Invasion of Hep-2 and HaCaT cell lines by *S. pseudintermedius*.** Human-derived Hep-2 and  
382 HaCaT cells were efficiently invaded by *S. pseudintermedius*, and invasion was dependent on Sps  
383 proteins. In addition, as reported for CPEK cells, internalization required the presence of Fn and  
384 involved the  $\alpha_5\beta_1$  integrin (see Figs. S1 and S2).

385 **Alterations to cell monolayers following internalization by *S. pseudintermedius*.** To investigate  
386 alterations to CPEK, Hep-2 and HaCaT cells following *S. pseudintermedius* invasion, cell  
387 monolayers were infected with *S. pseudintermedius* strain ED99 for 2 h prior to gentamicin  
388 treatment. Then the cells were incubated for 4 h and 36 h, fixed and analyzed for morphological  
389 changes by light microscopy. A remarkable difference in morphology was observed between  
390 infected and uninfected cell monolayers. Internalization of bacteria by CPEK cells caused cell  
391 detachment and a reduction of the cell density (Fig. 9A). Incubation of Hep-2 cells with strain ED99  
392 for 36 h resulted in rounding and detachment of the cells (see Fig. S3, panel A). In contrast, HaCaT  
393 cells showed a pattern similar to that exhibited by uninfected cells (see Fig. S3, panel C).

394 The assessment of the cell growth and survival of infected cells by the MTT assay showed  
395 that staphylococcal invasion substantially reduced the viability of CPEK (Fig. 9B) and Hep-2 (see  
396 Fig. S3, panel B) cells, whereas HaCaT cells survived to a level comparable to that of the  
397 uninfected cells (see Fig. S3, panel D). To further investigate the contribution of bacterial invasion  
398 to cell damage, all the cell lines were incubated with the *spsDspsL* double mutant. Both  
399 morphological observations and MTT assays showed that the double mutant did not affect the  
400 viability of cells.

401

## 402 **DISCUSSION**

403 In this paper we have analysed the molecular mechanism by which *S. pseudintermedius* adheres to  
404 and invades canine keratinocytes (CPEK cells) and the effects of internalization on the viability of  
405 the mammalian cells. We found that all strains of *S. pseudintermedius* tested invaded CPEK cells  
406 efficiently. Importantly, we found that both the cell wall-anchored surface proteins SpsD and SpsL



407 efficiently promoted invasion of strain ED99. Single mutants defective in either SpsD or SpsL alone  
408 showed no reduction in invasion. Only the double mutant lacking both proteins was defective.  
409 Conversely, both SpsD and SpsL promoted efficient uptake of the non-invasive surrogate host *L.*  
410 *lactis* when expressed ectopically from recombinant plasmids. Subdomains within SpsD and SpsL  
411 were expressed as recombinant proteins which allowed identification of regions with a high affinity  
412 for Fn and which also strongly inhibited bacterial invasion. Invasion of CPEK cells was dependent  
413 on the presence of Fn as demonstrated by the markedly reduced uptake upon removal of Fn from  
414 the cell culture medium (fetal bovine serum) and the restoration of invasion by supplementation  
415 with purified human Fn. We recognize the limitation of using human and bovine Fn to assess the  
416 role of this protein in bacterial invasion of a canine cell line. However, it should be noted that there  
417 is a high level of similarity between human, bovine and canine Fn (93-94% identity, 98%  
418 similarity) so that the use of human or bovine Fn is valid.

419 In *S. aureus* Fn-binding proteins FnBPA and FnBPB both promote invasion into mammalian cells  
420 where Fn acts as a bridge between the bacterial surface protein which binds to the N terminal N29  
421 domain by the tandem  $\beta$  zipper mechanism and the  $\alpha 5\beta 1$  integrin which recognizes an RGD motif  
422 within the C-terminal repeat 10 of Fn (18, 33). The finding that the N-terminal region of Fn and an  
423 RGD containing peptide inhibited *S. pseudintermedius* invasion into CPEK cells strongly suggests  
424 that the same mechanism is employed involving the Fn binding domains of SpsD and SpsL.  
425 Inhibition of invasion of CPEK cells by monoclonal antibodies recognizing epitopes in the human  
426  $\alpha 5\beta 1$  integrin strongly suggests that the canine CPEK cells express an immunocrossreactive  
427 integrin that is responsible for bacterial adhesion and invasion.

428 The Fn bridging mechanism for attachment to and invasion of mammalian cells results from  
429 integrin-initiated actin polymerization stimulated by receptor clustering and cell signalling events  
430 involving Src (34, 35). Here invasion of *S. pseudintermedius* was strongly reduced by the Src-  
431 specific inhibitors CGP77675 and PP-2 implying that similar mechanisms are responsible. Similar  
432 results were obtained when human Hep-2 epithelial cells and HaCaT keratinocytes were tested for

433 invasion by *S. pseudintermedius* ED99. However, certain differences were observed when  
434 compared to invasion of CPEK cells. A ten-fold smaller inoculum was needed for efficient invasion  
435 of Hep-2 cells compared to HaCaT and CPEK cells. We speculate that the differences in invasion  
436 efficiencies might be due to variations in the density of the  $\alpha 5\beta 1$  integrins although other factors  
437 could be involved. Together this data demonstrates that *S. pseudintermedius* employs a similar  
438 mechanism of host cell invasion as *S. aureus* that involves bacterial surface proteins binding to Fn  
439 and uptake mediated by integrin  $\alpha 5\beta 1$ .

440 Invasion of CPEK and Hep-2 cells resulted in cells detaching and losing viability whereas HaCaT  
441 cells remain unchanged. Thus in the first two cell lines invasion by *S. pseudintermedius* triggers a  
442 reduction in cell viability. Formaldehyde-killed bacterial cells were actively internalized by the  
443 mammalian cells suggesting that no active expression of invasogenic factors was necessary to  
444 achieve invasion. Conversely, the lack of effects on host cell survival by killed bacterial cells  
445 indicates that additional factors such as secreted toxins are required to induce cell death.

446 Membrane damaging toxins that are expressed by intracellular *S. aureus* are major factors in  
447 promoting apoptosis (36). *S. pseudintermedius* has the potential to express a bicomponent  
448 leukotoxin Luk-I which is similar to the Panton Valentine leucocidin (PVL) of *S. aureus* (37) as  
449 well as a homologue of  $\beta$ -toxin and a putative haemolysin (haemolysin III) (8). It can be  
450 hypothesized that at least one of these factors is responsible for inducing cell death in CPEK cells.  
451 Indeed, PVL facilitates escape of *S. aureus* from human keratinocyte endosomes and induces  
452 apoptosis (36) which might indicate a role here for Luk-I. Studies with mutants lacking one or more  
453 of the toxins will help clarify this point.

454 The initiation of the skin infection canine pyoderma is probably related to the ability of *S.*  
455 *pseudintermedius* to adhere to corneocytes on the surface of the *stratum corneum* as well as to  
456 invade the underlying keratinocytes. *S. pseudintermedius* adheres more strongly to corneocytes  
457 from regions of inflamed skin of dogs with atopic dermatitis than to non-inflamed areas suggesting

458 that ligands for bacterial surface protein adhesins are present at higher levels (31). Both SpsD and  
459 SpsO mediate bacterial adherence to canine corneocytes but the host ligands involved are not  
460 known (12). In addition, fibronectin is present in the *stratum corneum* of atopic human skin where  
461 it could provide an abundant ligand whereas it was not detected in healthy skin (32). Thus Fn could  
462 promote colonization of the *stratum corneum* as well as invasion of keratinocytes.

463 In conclusion, we have identified and characterized two fibronectin-binding proteins of *S.*  
464 *pseudintermedius* which are required for adhesion to and invasion of keratinocytes. An appropriate  
465 animal model will be required to assess the significance of SpsD and SpsL in the pathogenesis of  
466 canine pyoderma and to establish whether these antigens are suitable candidates for a  
467 multicomponent vaccine to combat the disease.

468

#### 469 ACKNOWLEDGEMENTS

470 We acknowledge funding from Fondazione CARIPLO (Grant Vaccines 2009-3546) to P.S. JRF  
471 received funding from Zoetis and Institute strategic funding from BBSRC. We would like to thank  
472 Dr. G. Guidetti of the Dipartimento di Biologia e Biotecnologie “L. Spallanzani,” University of  
473 Pavia, Italy for assistance and advice with fluorescence microscopy.

474

#### 475 REFERENCES

- 476 1. Perreten V, Kadlec K, Schwarz S, Grönlund Andersson U, Finn M, Greko C, Moodley  
477 A, Kania SA, Frank LA, Bemis DA, Franco A, Iurescia M, Battisti A, Duim B,  
478 Wagenaar JA, van Duijkeren E, Weese JS, Fitzgerald JR, Rossano A, Guardabassi L.  
479 2010. Clonal spread of methicillin-resistant *Staphylococcus pseudintermedius* in Europe and  
480 North America: an international multicentre study. J Antimicrob Chemother **65**:1145-1154.
- 481 2. Weese JS, and van Duijkeren E. 2010. Methicillin-resistant *Staphylococcus aureus* and  
482 *Staphylococcus pseudintermedius* in veterinary medicine. Vet Microbiol **140**:418-429.

- 483 3. **Maluping RP, Paul NC and Moodley A.** 2014. Antimicrobial susceptibility of methicillin-  
484 resistant *Staphylococcus pseudintermedius* isolated from veterinary clinical cases in the UK.  
485 Br J Biomed Sci **71**:55-57.
- 486 4. **Gerstadt K, Daly JS, Mitchell M, Wessolossky M and Cheeseman SH.** 1999.  
487 Methicillin-resistant *Staphylococcus intermedius* pneumonia following coronary artery  
488 bypass grafting. Clin Infect Dis **29**:218-219.
- 489 5. **Campanile F, Bongiorno D, Borbone S, Venditti M, Giannella M, Franchi C and**  
490 **Stefani S.** 2007. Characterization of a variant of the SCCmec element in a bloodstream  
491 isolate of *Staphylococcus intermedius*. Microb Drug Resist **13**:7-10.
- 492 6. **Kempker R, Mangalat D, Kongphet-Tran T and Eaton M.** 2009. Beware of the pet dog:  
493 a case of *Staphylococcus intermedius* infection. Am J Med Sci **338**:425-427.
- 494 7. **Stegmann R, Burnens A, Maranta CA and Perreten V.** 2010. Human infection  
495 associated with methicillin-resistant *Staphylococcus pseudintermedius* ST71. J Antimicrob  
496 Chemother **65**:2047-2048.
- 497 8. **Ben Zakour NL, Bannoehr J, van den Broek AH, Thoday KL and Fitzgerald JR.** 2011.  
498 Complete genome sequence of the canine pathogen *Staphylococcus pseudintermedius*. J  
499 Bacteriol **193**:2363-2364.
- 500 9. **Tse H, Tsoi HW, Leung SP, Urquhart IJ, Lau SK, Woo PC and Yuen KY.** 2011.  
501 Complete genome sequence of the veterinary pathogen *Staphylococcus pseudintermedius*  
502 strain HKU10-03, isolated in a case of canine pyoderma. J Bacteriol **193**:1783-1784.
- 503 10. **McEwan NA.** 2000. Adherence by *Staphylococcus intermedius* to canine keratinocytes in  
504 atopic dermatitis. Res Vet Sci **68**:279-283.
- 505 11. **McEwan NA, Kalna G and Mellor D.** 2005. A comparison of adherence by four strains of  
506 *Staphylococcus intermedius* and *Staphylococcus hominis* to canine corneocytes collected  
507 from normal dogs and dogs suffering from atopic dermatitis. Res Vet Sci **78**:193-198.

- 508 12. **Bannoehr J, Brown JK, Shaw DJ, Fitzgerald RJ, van den Broek AH and Thoday KL.**  
509 2012. *Staphylococcus pseudintermedius* surface proteins SpsD and SpsO mediate  
510 adherence to *ex vivo* canine corneocytes. *Vet Dermatol* **23**:119-124, e26. doi:  
511 10.1111/j.1365-3164.2011.01021.x.
- 512 13. **Latronico F, Moodley A, Nielsen SS and Guardabassi L.** 2014. Enhanced adherence of  
513 methicillin-resistant *Staphylococcus pseudintermedius* sequence type 71 to canine and  
514 human corneocytes. *Vet Res* **45**:70. doi: 10.1186/1297-9716-45-70.
- 515 14. **Geoghegan JA, Smith EJ, Speziale P and Foster TJ.** 2009. *Staphylococcus*  
516 *pseudintermedius* expresses surface proteins that closely resemble those from  
517 *Staphylococcus aureus*. *Vet Microbiol* **138**:345-352.
- 518 15. **Bannoehr J, Ben Zakour NL, Reglinski M, Inglis NF, Prabhakaran S, Fossum E,**  
519 **Smith DG, Wilson GJ, Cartwright RA, Haas J, Hook M, van den Broek AH, Thoday**  
520 **KL, Fitzgerald JR.** 2011. Genomic and surface proteomic analysis of the canine pathogen  
521 *Staphylococcus pseudintermedius* reveals proteins that mediate adherence to the  
522 extracellular matrix. *Infect Immun* **79**:3074-3086.
- 523 16. **Pietrocola G, Geoghegan JA, Rindi S, Di Poto A, Missineo A, Consalvi V, Foster TJ,**  
524 **Speziale P.** 2013. Molecular Characterization of the Multiple Interactions of SpsD, a  
525 Surface Protein from *Staphylococcus pseudintermedius*, with Host Extracellular Matrix  
526 Proteins. *PLoS One* **8**:e66901.
- 527 17. **Fraunholz M and Sinha B.** 2012. Intracellular *Staphylococcus aureus*: live-in and let die.  
528 *Front Cell Infect Microbiol* **2**:43. doi: 10.3389/fcimb.2012.00043.
- 529 18. **Sinha B, François PP, Nüsse O, Foti M, Hartford OM, Vaudaux P, Foster TJ, Lew DP,**  
530 **Herrmann M, Krause KH.** 1999. Fibronectin-binding protein acts as *Staphylococcus*  
531 *aureus* invasin via fibronectin bridging to integrin alpha5beta1. *Cell Microbiol* **1**:101-117.

- 532 19. **Peacock SJ, Foster TJ, Cameron BJ and Berendt AR.** 1999. Bacterial fibronectin-  
533 binding proteins and endothelial cell surface fibronectin mediate adherence of  
534 *Staphylococcus aureus* to resting human endothelial cells. *Microbiology* **145**:3477-3486.
- 535 20. **Fowler T, Wann ER, Joh D, Johansson S, Foster TJ and Höök M.** 2000. Cellular  
536 invasion by *Staphylococcus aureus* involves a fibronectin bridge between the bacterial  
537 fibronectin-binding MSCRAMMs and host cell beta1 integrins. *Eur J Cell Biol* **79**:672-679.
- 538 21. **Bannoehr J, Ben Zakour NL, Waller AS, Guardabassi L, Thoday KL, van den Broek**  
539 **AH, Fitzgerald JR.** 2007. Population genetic structure of the *Staphylococcus intermedius*  
540 group: insights into agr diversification and the emergence of methicillin-resistant strains. *J*  
541 *Bacteriology* **189**:8685–8692.
- 542 22. **Monk IR, Shah IM, Xu M, Tan MW and Foster TJ.** 2012. Transforming the  
543 untransformable: application of direct transformation to manipulate genetically  
544 *Staphylococcus aureus* and *Staphylococcus epidermidis*. *MBio* **3**(2). pii:e00277-11. doi:  
545 10.1128/mBio.00277-11.
- 546 23. **Speziale P, Visai L, Rindi S and Di Poto A.** 2008. Purification of human plasma  
547 fibronectin using immobilized gelatin and Arg affinity chromatography. *Nat Protoc* **3**:525-  
548 533.
- 549 24. **Zardi L, Carnemolla B, Balza E, Borsi L, Castellani P, Rocco M and Siri A.** 1985.  
550 Elution of fibronectin proteolytic fragments from a hydroxyapatite chromatography column.  
551 A simple procedure for the purification of fibronectin domains. *Eur J Biochem* **146**:571-579.
- 552 25. **Monk IR, Tree JJ, Howden BP, Stinear TP, Foster TJ.** 2015. Complete bypass of  
553 restriction systems for major *Staphylococcus aureus* lineages. *MBio* **6**(3). pii:e00308-15.  
554 doi: 10.1128/mBio.00308-15.
- 555 26. **Li MZ and Elledge SJ.** 2007. Harnessing homologous recombination *in vitro* to generate  
556 recombinant DNA via SLIC. *Nat Meth* **4**:251-256.

- 557 27. **Bae T and Schneewind O.** 2006. Allelic replacement in *Staphylococcus aureus* with  
558 inducible counter-selection. *Plasmid* **55**:58-63.
- 559 28. **Edwards AM and Massey RC.** 2011. Invasion of human cells by a bacterial pathogen. *J*  
560 *Vis Exp* (49). pii:2693. doi: 10.3791/2693.
- 561 29. **Akiyama SK and Yamada KM.** 1985. The interaction of plasma fibronectin with  
562 fibroblastic cells in suspension. *J Biol Chem* **260**:4492-4500.
- 563 30. **Pytela R, Pierschbacher MD and Ruoslahti E.** 1985. Identification and isolation of a 140  
564 kd cell surface glycoprotein with properties expected of a fibronectin receptor. *Cell* **40**:191-  
565 198.
- 566 31. **McEwan NA, Mellor D and Kalna G.** 2006. Adherence by *Staphylococcus intermedius* to  
567 canine corneocytes: a preliminary study comparing noninflamed and inflamed atopic canine  
568 skin. *Vet Dermatol* **17**:151-154.
- 569 32. **Cho SH, Strickland I, Boguniewicz M and Leung DY.** 2001. Fibronectin and fibrinogen  
570 contribute to the enhanced binding of *Staphylococcus aureus* to atopic skin. *J Allergy Clin*  
571 *Immunol* **108**:269-274.
- 572 33. **Edwards AM, Potter U, Meenan NA, Potts JR, Massey RC.** 2011. *Staphylococcus*  
573 *aureus* keratinocyte invasion is dependent upon multiple high-affinity fibronectin-binding  
574 repeats within FnBPA. *PLoS One* **6**:e18899. doi: 10.1371/journal.pone.0018899.
- 575 34. **Agerer F, Michel A, Ohlsen K and Hauck CR.** 2003. Integrin-mediated invasion of  
576 *Staphylococcus aureus* into human cells requires Src family protein-tyrosine kinases. *J Biol*  
577 *Chem* **278**:42524-42531.
- 578 35. **Fowler T, Johansson S, Wary KK and Höök M.** 2003. Src kinase has a central role in in  
579 vitro cellular internalization of *Staphylococcus aureus*. *Cell Microbiol* **5**:417-426.
- 580 36. **Chi CY, Lin CC, Liao IC, Yao YC, Shen FC, Liu CC, Lin CF.** 2014. Pantone-Valentine  
581 leukocidin facilitates the escape of *Staphylococcus aureus* from human keratinocyte  
582 endosomes and induces apoptosis. *J Infect Dis* **209**:224-235.

583 37. **Prevost G, Bouakham T, Piemont Y and Monteil H.** 1996. Characterisation of a  
584 synergohymenotropic toxin produced by *Staphylococcus intermedius*. FEBS Lett **381**:272.

585

#### 586 **FIGURE LEGENDS**

587 **FIG 1** Schematic diagram of SpsD and SpsL proteins from *S. pseudintermedius* ED99. The A  
588 domain of SpsD spans residues 37-519 following the secretory signal sequence S followed by a  
589 connecting domain C (residues 520-866) and a repeat region R. A sorting signal (SS:LPXTG motif,  
590 hydrophobic domain and positively charged residues) occurs at the extreme C-terminus. SpsL  
591 includes a signal sequence S at the N terminus followed by an A domain (residues 39-531), a  
592 domain containing seven tandem repeats (domain R, residues 543-818) and a C-terminal sorting  
593 signal (SS). The A domains of both proteins align with A domains of the MSCRAMM family of *S.*  
594 *aureus* surface proteins and each comprise three subdomains N1, N2 and N3 with N2 and N3  
595 predicted to form IgG-like folds. The A domains of SpsD and SpsL from ED99 have 30% identity  
596 and 50% similarity. The recombinant proteins are indicated along with ability of each truncate to  
597 bind to fibronectin.

598

599 **FIG 2** Dose-dependent binding of fibronectin to SpsD and SpsL fragments in an ELISA-type assay.  
600 Microtiter wells were coated with SpsD<sub>520-846</sub>, SpsD<sub>844-960</sub>, SpsL<sub>220-531</sub>, and SpsL<sub>538-823</sub>. The wells  
601 were probed with increasing amounts of Fn, followed by incubation with rabbit anti-Fn IgG and  
602 HRP-conjugated goat anti-rabbit IgG. The graph is representative of three experiments with each  
603 point representing the average of triplicate wells.

604

605 **FIG 3** Invasion of CPEK cell monolayers by *S. pseudintermedius* strains. *S. pseudintermedius* cells  
606 were incubated with CPEK cell monolayers. Extracellular bacteria were killed with gentamicin and  
607 internalized bacteria were quantified by plating lysates on BHI agar. The assay was performed



608 three times. Each point represents the average value for three replicas and error bars show the  
609 standard deviation. Statistically significant ( $P$ -value  $< 0.05$ , Student's  $t$ -test) differences in values  
610 compared with the control value (*S. aureus* Cowan 1) are indicated by an asterisk. The absence of  
611 intracellular bacteria in cell cultures was established by lysing samples of the confluent monolayers  
612 and plating on BHI agar prior to staphylococcal inoculation.

613

614 **FIG. 4.** Role of soluble fibronectin on invasion by *S. pseudintermedius*. A) To evaluate the effect of  
615 endogenous fibronectin, the invasion assay was performed in the presence of 10% FBS (a), 10 %  
616 Fn-depleted FBS (b), 10 % Fn-depleted FBS + 1 $\mu$ g/ml soluble human plasma Fn (c), and in the  
617 absence of FBS (d). Bacteria were incubated with CPEK cell monolayers and internalized bacteria  
618 were quantified as described in Fig. 3. Invasion is expressed as a percentage of that observed in the  
619 presence of 10% whole FBS (control:  $2 \times 10^5$  CFU). Each point represents the average value for  
620 three replicas and error bars represent means  $\pm$  S.D. of three independent experiments performed in  
621 triplicate. Statistically significant ( $P$ -value  $< 0.01$ , Student's  $t$ -test) differences in values compared  
622 with control value in the presence of FBS is indicated by an asterisk. B) To determine the effect of  
623 the N29 fragment, staphylococci were incubated with increasing concentrations of N29 or 650 nM  
624 GBD for 30 min at 22°C. Bacteria were then added to CPEK cell monolayers and incubated at  
625 37°C for 2 h and internalized bacteria were quantified as described in Fig. 3. Invasion is expressed  
626 as a percentage of that observed in the absence of inhibitors (control:  $2.5 \times 10^5$  CFU). Error bars  
627 represent means  $\pm$  S.D. of three independent experiments performed in triplicate.

628

629 **FIG 5** Invasion of CPEK cell monolayers by *S. pseudintermedius* and its mutants. A) Expression of  
630 SpsD and SpsL proteins. Cell wall proteins from the the wild type and mutants were solubilized  
631 with lysostaphin, separated by SDS-PAGE and analyzed by Western immunoblotting using mouse  
632 anti-SpsD or anti-SpsL and HRP-labeled rabbit anti-mouse IgG. B) *S. pseudintermedius* wild-type  
633 and  $\Delta$ *spsD*  $\Delta$ *spsL* were incubated with CPEK cell monolayers, and internalized bacteria quantified

634 as reported in Fig. 3. Error bars are  $\pm$  S.D. of the mean of three independent determinations  
635 performed in triplicate. An asterisk indicates a significant difference ( $P$ -value  $< 0.05$ , Student's  $t$ -  
636 test) compared with the control (invasion with the wild type strain). C) Fluorescent microscopy  
637 investigating the contribution of SpsD or SpsL to interactions with CPEK cells. Confluent CPEK  
638 monolayers were incubated with calcein-AM labeled *S. pseudintermedius* to allow internalization,  
639 washed with PBS and counterstained with ethidium bromide. Green fluorescence represents  
640 intracellular staphylococci and red fluorescence extracellular bacteria. Scale bar = 40  $\mu$ m.

641

642 **FIG 6** Invasion of CPEK cell monolayers by *L. lactis*. A) Expression of SpsD and SpsL by *L.*  
643 *lactis*. Cell wall proteins were solubilized with mutanolysin and lysostaphin, separated by SDS-  
644 PAGE and analyzed by Western immunoblotting using mouse anti-SpsD or anti-SpsL as primary  
645 antibodies and HRP-labeled rabbit anti-mouse IgG. B) CPEK invasion by *L.lactis* expressing SpsD  
646 or SpsL. *L. lactis* were incubated with CPEK cell monolayers and internalized bacteria measured  
647 as indicated above. Error bars are  $\pm$  S.D. of the mean of three independent determinations  
648 performed in triplicate. An asterisk indicates a significant difference ( $P$ -value  $< 0.05$ , Student's  $t$ -  
649 test) compared with *L. lactis* pOri23::*spsD* or pOri23::*spsL*. C) Fluorescent imaging investigating  
650 the contribution of SpsD or SpsL to interactions with CPEK cell monolayers. Confluent CPEK  
651 monolayers were incubated with calcein-AM-labeled *L. lactis* to allow internalization.  
652 Fluorescence was visualized as in Fig. 5. Scale bar = 40  $\mu$ m.

653

654 **Fig 7** Effect of SpsD and SpsL fragments on invasion of CPEK cells by *S. pseudintermedius*. CPEK  
655 cell monolayers were incubated with increasing concentrations of SpsD<sub>164-523</sub>, SpsD<sub>520-846</sub> or  
656 SpsD<sub>844-960</sub> (A), SpsL<sub>220-531</sub> or SpsL<sub>538-823</sub> (B) prior to addition of bacteria. Invasion is expressed as a  
657 percentage of that observed in the absence of potential inhibitors (control:  $2.2 \times 10^5$  CFU). Error bars  
658 are  $\pm$  S.D. of the mean of three independent determinations performed in triplicate. Statistically  
659 significant differences are indicated (Student's two-tailed  $t$ -test,  $*P < 0.05$ ,  $**P < 0.001$ ).

660

661 **FIG 8** A) Effect of anti-integrin antibodies on invasion of CPEK cells by *S. pseudintermedius*.  
662 CPEK monolayers were incubated with antibodies against  $\alpha_5\beta_1$  and  $\alpha_v\beta_3$  integrins prior to the  
663 addition of bacteria. After incubation internalized bacteria were quantified as described above.  
664 Invasion is expressed as the percentage of that observed in the absence of antibodies (control:  
665  $2.8 \times 10^5$  CFU). Error bars represent the mean  $\pm$  S.D. of three independent determinations performed  
666 in triplicate. Statistically significant differences are indicated (Student's two-tailed *t*-test,  $*P <$   
667 0.05). The inset shows expression of  $\alpha_5\beta_1$  integrin by CPEK cells by staining with  
668 immunofluorescent antibodies that specifically bind to the  $\alpha_5$  subunit of the  $\alpha_5\beta_1$  integrin. Scale bar  
669 = 40  $\mu$ m. B). Effect of an RGD containing peptide on invasion of CPEK cells by *S.*  
670 *pseudintermedius* - CPEK cells were incubated with increasing concentrations of the RGDS or  
671 RGEs peptides prior to addition of bacteria. After incubation internalized bacteria were quantified  
672 as described above. Invasion is expressed as a percentage of that observed in the absence of  
673 peptides (control:  $2.3 \times 10^5$  CFU). Error bars represent the mean  $\pm$  S.D. of three independent  
674 determinations performed in triplicate. C) Effect of kinase inhibitors on invasion of CPEK cells by  
675 *S. pseudintermedius* - CPEK cells were exposed to genistein, CGP77675, PP2 and PP3, wortmannin  
676 and cytochalasin D for 1 h before addition of bacteria. Invasion assays were performed on inhibitor-  
677 treated cells three times with similar results. Invasion is expressed as a percentage of that observed  
678 in the absence of inhibitors (control:  $2.1 \times 10^5$  CFU). Error bars represent the mean  $\pm$  S.D. of three  
679 independent determinations performed in triplicate. Statistically significant differences are indicated  
680 (Student's two-tailed *t*-test,  $*P < 0.05$ ,  $**P < 0.001$ ).

681

682 **FIG 9** Effects on CPEK cells following invasion. A) Alterations to CPEK monolayers after  
683 infection with *S. pseudintermedius* and the double  $\Delta$ *spsD/spsL* mutant. Monolayers were infected  
684 with *S. pseudintermedius* prior to gentamicin treatment. Then the cells were incubated for 4 h and

685 36 h, stained with Giemsa and observed for morphological changes by light microscopy. Scale bar  
 686 = 200  $\mu$ m. B) Assessment of survival of infected cells. Confluent CPEK cells were infected for 2h  
 687 with *S. pseudintermedius* ED99 or the double  $\Delta$ *spsD/spsL* mutant and then examined at 4h and 36  
 688 h after infection for viability by the MTT assay. Viability was assessed as the percentage of  
 689 absorbance at 575 nm of treated cells relative to that of solvent-treated controls. Error bars represent  
 690 the mean  $\pm$  S.D. of three independent determinations performed in triplicate. Statistically significant  
 691 differences are indicated (Student's two-tailed *t*-test, \**P* < 0.05).

692

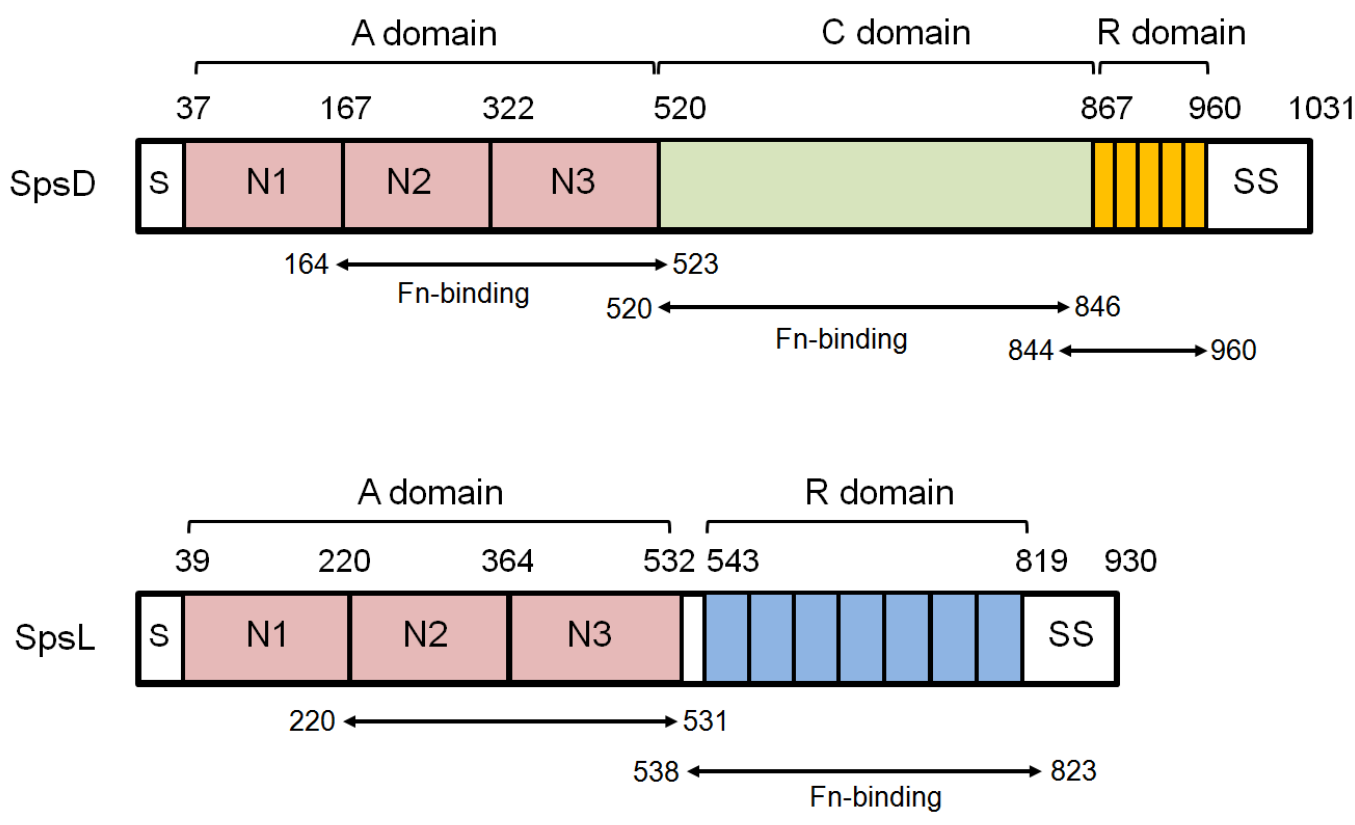
693 **TABLE 1** Plasmids used for the construction of *spsD* and *spsL* null mutants

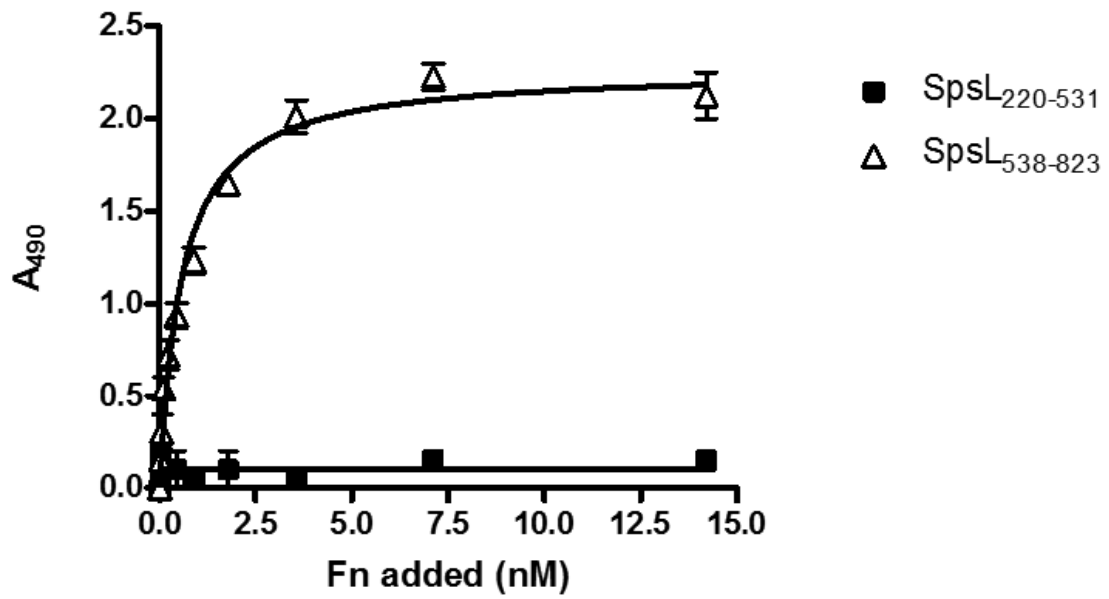
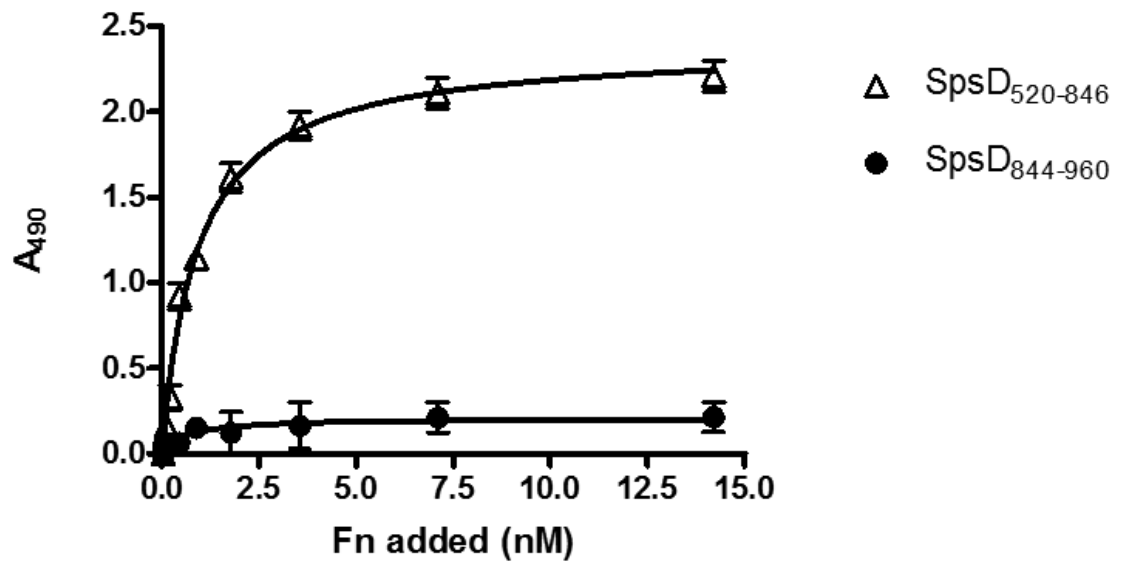
Strain or Plasmid	Description	Reference
pIMAY	Thermosensitive plasmid for allelic exchange	(21)
pIMAY $\Delta$ <i>spsD</i>	pIMAY with fragments flanking <i>spsD</i>	This paper
pIMAY-Z	pIMAY derivative with a constitutive <i>lacZ</i> marker	(25)
pIMAY-Z $\Delta$ <i>spsL</i>	pIMAY-Z with fragments flanking <i>spsL</i>	This paper

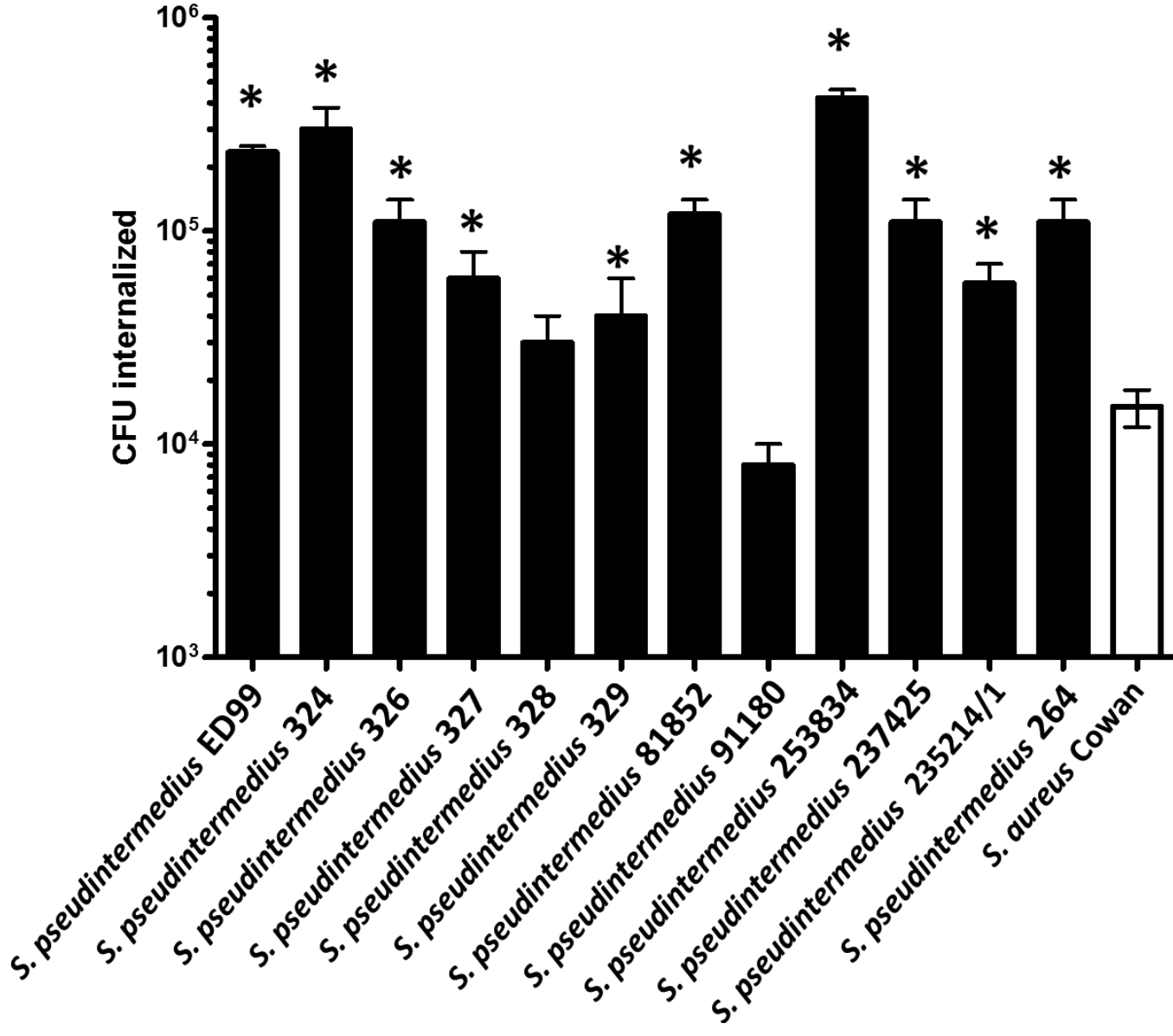
694

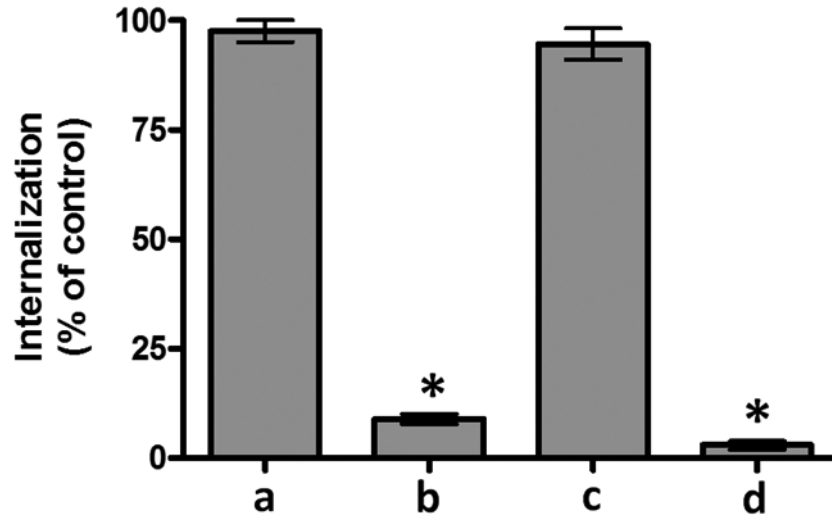
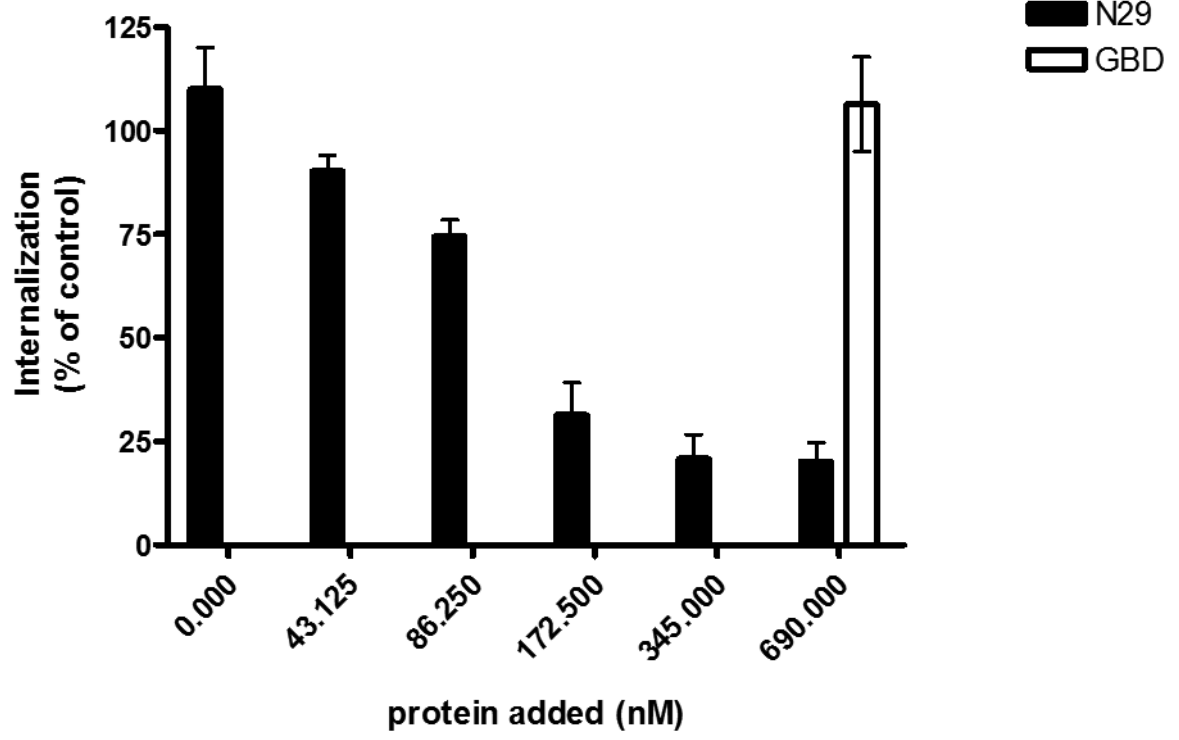
695

696

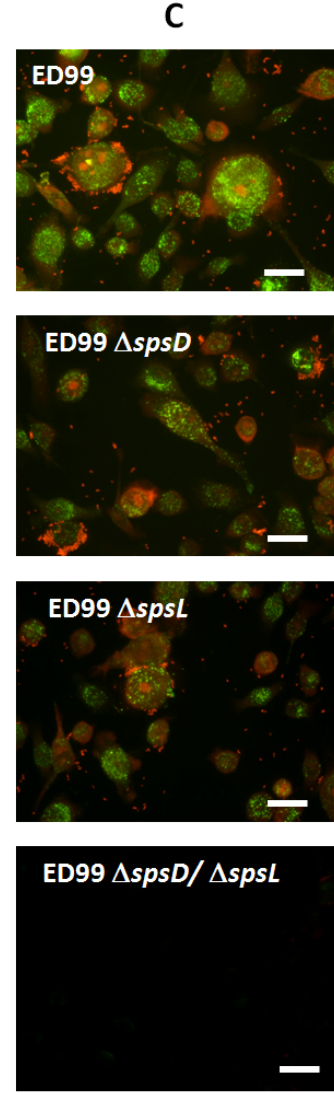
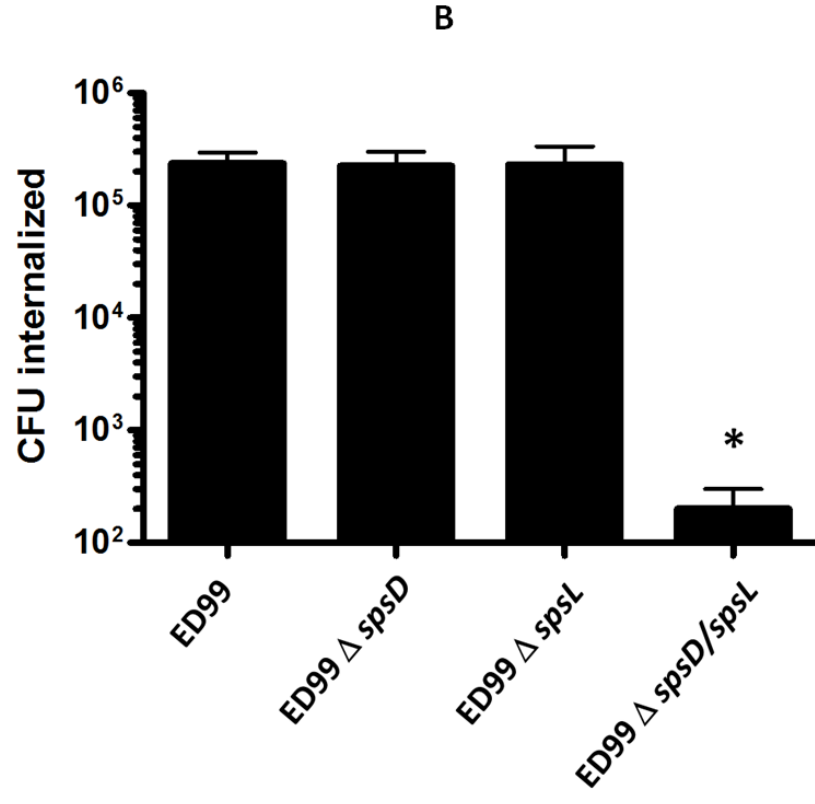
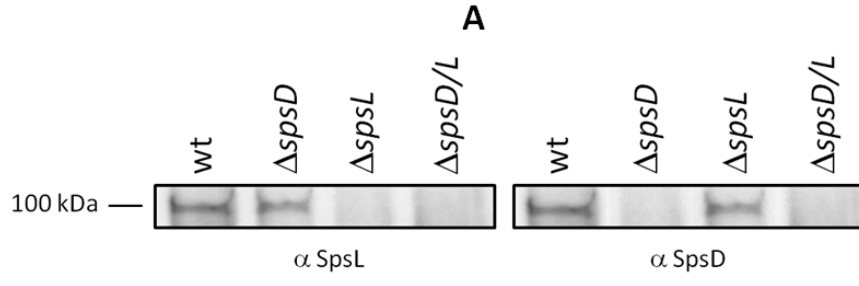


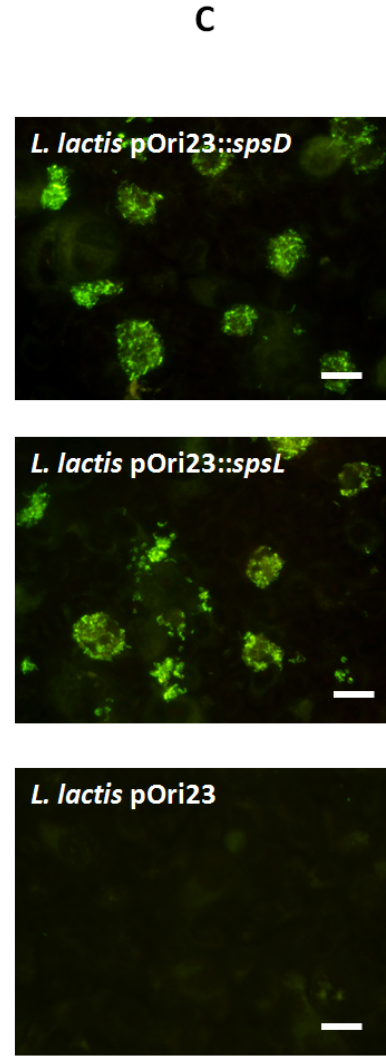
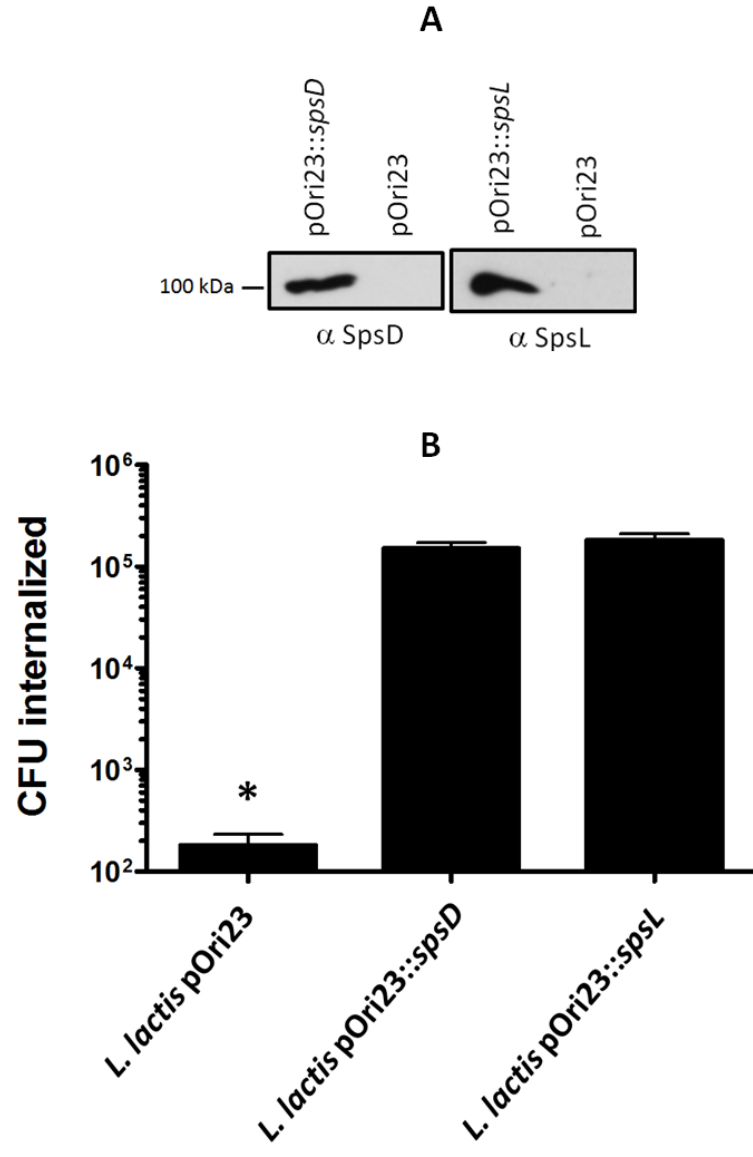
**A****B**



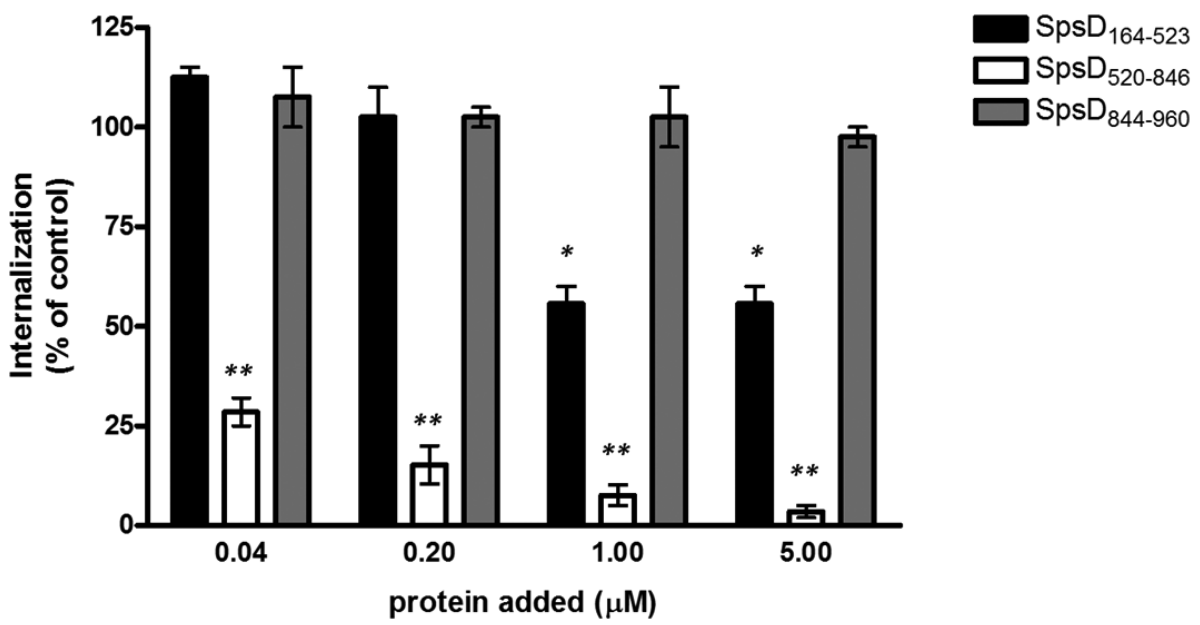
**A****B**







A



B

